Luttinger liquids with curvature: Density correlations and Coulomb drag effect

D. N. Aristov*
Institut für Theorie der Kondensierten Materie, Universität Karlsruhe, 76128 Karlsruhe, Germany
and Center for Functional Nanostructures, Universität Karlsruhe, 76128 Karlsruhe, Germany
(Received 20 February 2007; revised manuscript received 14 May 2007; published 16 August 2007)

We consider the effect of the curvature in fermionic dispersion on the observable properties of Luttinger liquid (LL). We use the bosonization technique where the curvature is irrelevant perturbation, describing the decay of LL bosons (plasmon modes). When possible, we establish the correspondence between the bosonization and the fermionic approach. We analyze modifications in density correlation functions due to curvature at finite temperatures, T. The most important application of our approach is the analysis of the Coulomb drag by small momentum transfer between two LLs, which is only possible due to curvature. Analyzing the ac transconductivity in the one-dimensional drag setup, we confirm the results by Pustilnik *et al.* for T dependence of drag resistivity, $R_{12}\sim T^2$ at high and $R_{12}\sim T^5$ at low temperatures. The bosonization allows for treating both intra- and interwire electron-electron interactions in all orders, and we calculate exact prefactors in the low-T drag regime. The crossover temperature between the two regimes is $T_1\sim E_F\Delta$, with Δ relative difference in plasmon velocities. We show that $\Delta\neq 0$ even for identical wires, due to lifting of degeneracy by interwire interaction, U_{12}, leading to crossover from $R_{12}\sim U_{12}^2T^2$ to $R_{12}\sim T^5/U_{12}$ at $T\sim U_{12}$.

DOI: 10.1103/PhysRevB.76.085327 PACS number(s): 73.63.Nm, 71.10.Pm, 72.15.Nj, 73.23.Ad

I. INTRODUCTION

The effects of the curvature of fermionic dispersion for the observables in strongly correlated one-dimensional (1D) fermionic systems were discussed by several groups recently.[1–7] One physical effect, which probes both the curvature and interactions is the Coulomb drag effect. In a typical experimental setup, this effect is observed as nonzero drag resistivity, $R_{12}=V_2/I_1$, with a dc current I_1 flowing in the "active" wire and the voltage bias V_2 per unit length applied to the second "passive" wire in order to assure $I_2=0$; see the review articles in Ref. 8.

It is generally agreed that the principal source of the drag effect is the particle-hole asymmetry of the electronic system. This was established in various works considering electrons in higher spatial dimensions, $D>1$, both in the absence of magnetic field[9] and in the presence of it (see Ref. 10 and references therein). It was shown that the leading contribution to the drag effect is obtained in the second order of the interwire interaction U_{12} and is schematically depicted by the Feynman graph in Fig. 2. This contribution corresponds to the virtual processes away from the Fermi surface and is ultimately determined by the curvature of the electronic dispersion.

One naturally would expect that the curvature should be also responsible for the drag effect in one spatial dimension (1D). However, the first study of the drag effect in 1D was devoted to a different mechanism,[11] specific for 1D and requiring some additional conditions, we return to it below. The study of the drag effect in 1D due to curvature of electronic dispersion was initiated only recently by Pustilnik *et al.*[1] The reason is that the drag effect depends both on the curvature and the fermionic interaction, whereas it is known that the interaction is very important in 1D and ultimately leads to the notion of Luttinger liquid. The possibility to find a complete solution, i.e., Luttinger liquid, for the interacting system lies in the crucial simplification of the theory—the linearization of the fermionic dispersion around the Fermi energy. In most cases it is an innocent procedure and does not influence the final result. The Coulomb drag effect is one example where this usual theoretical trick with linearization leads to the immediate disappearance of the observable quantity in question. In their work,[1] Pustilnik *et al.* (see also Ref. 5) used the fermionic formalism, and found the drag effect as the function of temperature, for different regimes. Restricting themselves to the lowest order of interwire, as well as intrawire interactions, they showed that $R_{12}\propto T^2$ for equal wires and $R_{12}\propto T^5$ for nonequal wires. In this work we check their results by another method and extend their treatment beyond the lowest order of perturbation theory (PT) in fermionic interactions.

To this end, we use the traditional tool for studying the effects of interaction in 1D, known as the bosonization technique, which is devised for effective resummation of the appearing series in PT.[12] Employing the bosonization we take into account the inter- and intrawire interactions in all orders, whereas the curvature of fermionic dispersion is treated as perturbation. We show that it suffices to consider fourth order in curvature when calculating low-temperature drag effect. At higher temperatures we perform the resummation of most singular contributions in PT in curvature, incorporating free-fermion results into bosonization language. In this sense, our method is complementary to the analysis in Ref. 1 where the curvature was treated exactly and the interactions in the lowest necessary order.

The issue of the curvature of fermionic dispersion in the bosonization technique was rarely discussed previously. Therefore, although we are ultimately interested in the drag effect, we develop a systematic approach to Luttinger liquid with curvature. It was shown long ago[13,14] that the curvature corresponds to the cubic terms in bosonic densities (plasmon modes) of so-called right- and left-moving fermions near two Fermi points $\pm k_F$, respectively. The appearance of these cubic terms corresponds to the decay of bosons (plasmons) and was previously derived in two ways via operator identities.

We suggest yet another explanation for the appearance of the cubic terms in the theory, an explanation referring to Green's function formalism and more pertinent to our discussion of Coulomb drag. Besides that we discuss the modification of the current operator, dynamic density correlations in isolated wires, and the light-cone singularities at finite temperatures T. Keeping T finite is important for our calculation, as the drag effect is only due to inelastic processes of fermionic interaction, and hence vanishes at $T=0$. We use the Kubo formalism, which technically delivers the optical transconductivity, $\sigma_{ij}(\omega)$, in a one-dimensional system of two wires, and eventually extract the dc drag resistivity, $\sigma_{ij}^{-1}(0)$. Given our assumption of clean Luttinger liquids, it is a delicate procedure and we discuss it in detail.

The plan for the paper is as follows. We set up the problem and discuss the identification of fermionic curvature with decay of plasmon modes in Sec. II. The form of density correlation functions is discussed in Sec. III; we show the correspondence between fermionic approach and bosonization here. The bosonization expression for current and conductivity for one wire is discussed in Sec. IV. The transconductivity matrix for two wires is considered in Sec. V, and the drag coefficient is obtained for the relatively simple case of nonequal wires. The analysis of nearly equal wires is performed separately, in most technically involved Sec. VI, where the final results for R_{12} in low temperature regime are discussed. We present our summary and conclusions in Sec. VII.

II. SETTING UP THE PROBLEM

A. Hamiltonian

We consider spinless (spin-polarized) electrons in two wires, with the forward-scattering short-range interaction both inside and between the wires. The electrons in the ith wire $(i=1,2)$ are conventionally subdivided into right- and left-going species, centered around corresponding Fermi momenta, $k_{Fi}=\pi n_i$, with the fermionic density n_i. We go beyond the linearized spectrum approximation, keeping quadratic terms in dispersion.

As usual, we decompose the fermionic operator into "slowly oscillating" chiral components

$$\psi(x) = e^{ik_F x}\psi_R(x) + e^{-ik_F x}\psi_L(x), \tag{1}$$

so that the smooth part of the fluctuating fermionic density is

$$\rho(x) = \psi_R^\dagger(x)\psi_R(x) + \psi_L^\dagger(x)\psi_L(x). \tag{2}$$

Our Hamiltonian is given by four terms:

$$\mathcal{H} = \int dx(H_1 + H_2 + H_{12} + H_{cur}),$$

with the linearized interacting fermions in individual wires

$$H_{j=1,2} = -iv_{Fj}\psi_{Rj}^\dagger\partial_x\psi_{Rj} + iv_{Fj}\psi_{Lj}^\dagger\partial_x\psi_{Lj} + U_j\rho_j^2(x)/2, \tag{3}$$

forward-scattering interaction between wires

$$H_{12} = U_{12}\rho_1(x)\rho_2(x), \tag{4}$$

and the terms describing the curvature of fermionic dispersion

$$H_{cur} = \sum_{j=1,2}\frac{1}{2m_j}[\psi_{Rj}^\dagger(i\partial_x)^2\psi_{Rj} + \psi_{Lj}^\dagger(i\partial_x)^2\psi_{Lj}]. \tag{5}$$

The bosonization approach to the above system is the application of the important representation of 1D chiral fermions as

$$\psi_{Rj} = \frac{1}{\sqrt{2\pi\Lambda}}e^{i\phi_{Rj}}, \quad \psi_{Lj} = \frac{1}{\sqrt{2\pi\Lambda}}e^{-i\phi_{Lj}}, \tag{6}$$

with Λ the ultraviolet cutoff. Here the bosonic fields $\phi_{R(L),j}=\phi_j \mp \theta_j$, with primary field ϕ_j and its canonically conjugated momentum $\Pi_j=\pi^{-1}\partial_x\theta_j$ satisfying $[\phi_j(x),\Pi_l(y)]=i\delta_{jl}\delta(x-y)$.

In this bosonization notation,[12] the Hamiltonian of the system is rewritten as follows:

$$\mathcal{H} = \int dx(H_1 + H_2 + H_{12} + H_{cur}), \tag{7}$$

$$H_{i=1,2} = \frac{1}{2\pi}[v_{iJ}(\partial_x\theta_i)^2 + v_{iN}(\partial_x\phi_i)^2], \tag{8}$$

$$H_{12} = \frac{U_{12}}{\pi^2}\partial_x\phi_1\partial_x\phi_2,$$

$$H_{cur} = \frac{1}{6\pi m_1}\partial_x\phi_1[3(\partial_x\theta_1)^2 + (\partial_x\phi_1)^2] + (1 \leftrightarrow 2). \tag{9}$$

Here and below I use the shorthand notation $\partial_x\phi_1=\partial\phi_1(x)/\partial x$, etc. The electronic density operator in Eq. (7) is given by $\rho_i=\partial_x\phi_i/\pi$. We follow the notation by Haldane, with $v_{iJ}=v_{Fi}=k_{Fi}/m_i$, $v_{iN}=v_{Fi}+U_i/\pi$. In the absence of H_{12}, H_{cur}, the dispersion of (plasmon) excitations is $\varepsilon_i(q)=v_i|q|$, where $v_i^2=v_{iJ}v_{iN}$. The strength of the intrawire interactions may be encoded in the Luttinger parameters, $K_i=\sqrt{v_{iJ}/v_{iN}}$; it is convenient also to define the dimensionless interwire interaction, $u=\pi^{-1}U_{12}/\sqrt{v_{1N}v_{2N}}$.

It is seen that the Hamiltonian (7) contains an exactly solvable quadratic-in-bosons part $H_1+H_2+H_{12}$ and the curvature acts as the interaction.

B. Curvature as interaction

In bosonization, the normally ordered parts of chiral fermionic densities become

$$R_j \equiv \psi_{Rj}^\dagger\psi_{Rj}, \quad L_j \equiv \psi_{Lj}^\dagger\psi_{Lj}, \tag{10}$$

with $\rho_j=R_j+L_j=\pi^{-1}\partial_x\phi_j$. The main statement of (Abelian) bosonization, dating back to Tomonaga,[15] is that the free chiral fermions with linear dispersion are equivalent to the quadratic form in chiral densities: $-i\psi_R^\dagger\partial_x\psi_R=\pi R^2$. Tomonaga established this relation, studying the equation of motion for the chiral density R with the fermionic Hamiltonian with linear dispersion. This observation was later corroborated by Schick,[14] who found that similar consideration with the quadratic fermionic dispersion yields another important relation:

FIG. 1. Feynman diagrams representing nonlinear response of the fermionic system. Two three-tail fermion loops correspond to a boson decay process, see the text for discussion.

$$\psi_R^\dagger \frac{(i\partial_x)^2}{2m}\psi_R = \frac{2\pi^2}{3m}R^3. \tag{11}$$

Another derivation of Eq. (11) was shown in the paper by Haldane,[13] who started with the fermion representation (6). Note that using Eq. (6), one arrives also to the term in the Hamiltonian, which constitutes a full derivative, $\sim\partial_x^2\phi_R\partial_x\phi_R \sim \partial_x(R^2)$, which does not contribute to the dynamics. Confining oneself with the quadratic terms in the fermionic dispersion, one obtains nothing beyond the terms R^2+L^2 and R^3+L^3 in the bosonization language. The stability issue for the cubic action is briefly discussed in the next section.

Keeping in mind a problem of drag effect, let us provide yet another argument verifying the form of the curvature term in bosonization. It is well-known that the multitail fermionic loop diagrams in one spatial dimension are exactly zero for the linear dispersion law. This statement is known as the higher-loop cancellation theorem after the work by Dzyaloshinskii and Larkin.[16] One can show, however, that the presence of the curvature in fermionic dispersion leads to a generally nonzero value for the processes given by the triangle diagram. The expression for this diagram, characterized by three external vertices, can be easily calculated at $T=0$ as

$$\mathcal{T} = \frac{q_1q_2q_3\left[\sum_{i=1}^{3}\Lambda(\omega_i,q_i)\right]}{(\omega_1q_2-\omega_2q_1)^2-(q_1q_2q_3/2m)^2}, \tag{12}$$

$$\Lambda(\omega,q) = \frac{1}{2\pi}\ln\frac{\omega-v_Fq+q^2/2m}{\omega-v_Fq-q^2/2m}, \tag{13}$$

with $q_3=q_1+q_2$, $\omega_3=\omega_1+\omega_2$ (see also Ref. 17). One can check that $\mathcal{T}$ vanishes in the limit $m\to\infty$. Expanding Eq. (12) to the leading order of m^{-1}, one obtains the structure

$$\frac{1}{2\pi m}\frac{q_1}{v_Fq_1-\omega_1}\frac{q_2}{v_Fq_2-\omega_2}\frac{q_3}{v_Fq_3-\omega_3}, \tag{14}$$

which corresponds to three density correlators for the linear spectrum, $(2\pi)^{-1}q/(v_Fq-\omega)$, attached to the above vertex, $2\pi^2/(3m)$; factor $3!=6$ comes from symmetrization. Schematically, it is shown as Feynman diagrams in Fig. 1, where fermion Green's functions are shown by lines with arrows, and double lines represent bosonic Green's functions (21). Note that the leading-order drag diagram is given by the "two triangles" fermionic diagrams in Fig. 2, with wavy lines standing for U_{12}.[9,10] Comparing it to Fig. 1 we see that the drag coefficient should correspond to the "two stars" bosonic

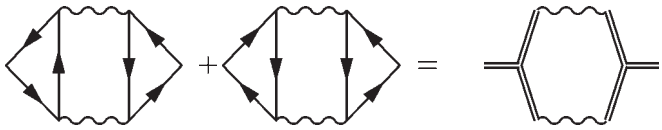

FIG. 2. First Coulomb drag diagrams in the fermionic formalism and their bosonization counterpart, see the text for discussion.

diagram in the right-hand side of Fig. 2. Further observing that interwire interaction, U_{12}, is exactly included into the Luttinger liquid formalism, Eq. (7), we eventually arrive at the diagrams depicted in Fig. 3 below. Note that passing from Fig. 2 to Fig. 3 corresponds to the screening of interwire interaction; see, e.g., Kamenev and Oreg.[9] The RPA resummation in the case of LL gives an exact result; however, the simplest bosonic diagram in Fig. 2 corresponds to the optical transconductivity, rather than to dc drag effect, as will be shown below. Before considering a general case of two different wires, let us discuss the modification of density correlations in one wire with the curvature term.

III. DENSITY CORRELATIONS

Let us first discuss the density correlation function for one wire, with and without the Luttinger-liquid type interaction. Such an analysis was previously done in Refs. 3 and 4, we extend it for the case $T\neq 0$ in all orders of intrawire interaction. The bosonized Hamiltonian reads as

$$\mathcal{H} = \int dx(H_0+H_{cur}), \tag{15}$$

$$H_0 = \frac{1}{2\pi}[v_J(\partial_x\theta)^2+v_N(\partial_x\phi)^2] \tag{16}$$

$$= \pi v_F(R^2+L^2)+\frac{U}{2}(R+L)^2, \tag{17}$$

$$H_{cur} = \frac{1}{6\pi m}\partial_x\phi[3(\partial_x\theta)^2+(\partial_x\phi)^2] \tag{18}$$

$$= \frac{2\pi^2}{3m}(R^3+L^3). \tag{19}$$

The commutation rules for the chiral densities are

$$[R(x),R(y)] = -[L(x),L(y)] = \frac{i}{2\pi}\partial_x\delta(x-y). \tag{20}$$

Our choice of the interaction in the form $U(R+L)^2$ corresponds to the case $g_4=g_2$ in the more general form of the Hamiltonian $g_4(R^2+L^2)+2g_2RL$.

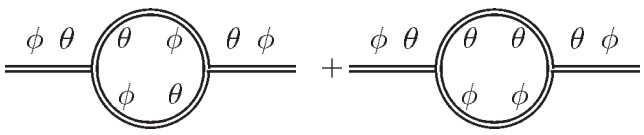

FIG. 3. Two boson diagrams for ac conductivity, obtained with the use of continuity relation and equivalent to Fig. 4.

A. Free fermions

In the absence of the mixing interaction term *URL* in Eq. (17), each chiral component is considered separately. In the absence of the curvature, $1/m=0$, the bare boson retarded right (left) Green's function is independent of temperature and given by

$$g^{(0)}_{R(L)} = \frac{1}{2\pi} \frac{q}{qv_F \mp (\omega + i0)}, \tag{21}$$

with δ-function spectral weight.

Importantly, in this free case we know the exact expression for the correlation function of the right (left) moving densities. The retarded (right) density propagator $\chi(\omega,q)$ can be calculated at nonzero temperature as the fermionic loop diagram,

$$\chi = \int \frac{dk}{4\pi} \frac{\tanh(\varepsilon_k/2T) - \tanh(\varepsilon_{k+q}/2T)}{\omega + \varepsilon_k - \varepsilon_{k+q} + i0}, \tag{22}$$

with $\varepsilon_k = v_F k + k^2/2m$. Neglecting the terms of order of $T/(mv_F^2)$, we get

$$\mathrm{Im}\,\chi = \frac{m}{4q} \frac{\sinh(\omega/2T)}{\cosh\left(\frac{qv_F(\Omega-1)}{4T}\right)\cosh\left(\frac{qv_F(\Omega+1)}{4T}\right)}, \tag{23}$$

$$\chi = \frac{q}{4\pi w_q}\left[\psi\left(\frac{1}{2} - i\frac{|qv_F|(\Omega-1)}{4\pi T}\right) - \psi\left(\frac{1}{2} - i\frac{|qv_F|(\Omega+1)}{4\pi T}\right)\right], \tag{24}$$

$$\Omega = (\omega - qv_F)/w_q, \quad w_q = q^2/(2m), \tag{25}$$

with $\psi(x)$ the digamma function. Restoring the real part of χ we used the rule

$$i\tanh z \to -\frac{2}{\pi}\psi\left(\frac{1}{2} - i\frac{z}{\pi}\right)$$

for the analytic function in the upper semiplane of z. In the limit of zero temperature we obtain

$$\mathrm{Im}\,\chi = \frac{m}{2q}\Theta(1 - |\Omega|), \tag{26}$$

$$\chi = \frac{q}{4\pi w_q} \ln \frac{\omega - qv_F - w_q + i0}{\omega - qv_F + w_q + i0}, \tag{27}$$

with the step-function $\Theta(x)=1$ at $x>0$.

Let us now discuss how these exact expressions relate to the bosonization theory. Formally, the curvature term H_{cur} has a scaling dimension 3, which is strongly irrelevant. The common wisdom then would prescribe to treat it in the lowest order of perturbation theory (PT) in the infrared limit, $q,\omega \to 0$. Comparing Eq. (27) and the bosonization expression (21), one can see that the δ function is a good approximation for the spectral weight in this limit. However, the lowest PT contribution, with two bosons in the intermediate state, leads to the self-energy part of the form

$$\Sigma = 2\pi \frac{q}{12m^2} \frac{q^2 + (2\pi T/v_F)^2}{qv_F - \omega - i0}. \tag{28}$$

Note that in a quite unusual way[18] the spectral weight $\mathrm{Im}\,\Sigma(\omega,q)$ is located exactly at the "light cone" of the bare spectrum, $\omega - qv_F = 0$. The Dyson equation, $g_R^{-1} = (g_R^{(0)})^{-1} - \Sigma$, reads as

$$g_R^{-1} = 2\pi\left[\frac{qv_F - \omega}{q} - \frac{q}{12m^2}\frac{q^2 + (2\pi T/v_F)^2}{qv_F - \omega}\right]. \tag{29}$$

It means that instead of previous single pole $\omega = qv_F$, we have two poles separated by a distance $\sim m^{-1} q \max[q,T]$.

Now we compare Eq. (29) with Eq. (24) by expanding χ^{-1} in powers of m^{-1}. We find that Eq. (29) is reproduced by Eq. (24) in the order m^{-2}. It suggests that bosonization produces a correct *asymptotic* series in m^{-1}, but at the energies close to "light-cone" condition, an ever increasing number of PT corrections should be taken into account, to arrive at the exact answer (24).

Interestingly, the bosonization predicts also that the fermionic interaction of the form $g_4(R^2+L^2)$, i.e., with $g_2=0$, results only in the shift of the Fermi velocity, and therefore the spectral weight χ has the previous form (24) except for the change, $v_F \to v_F + g_4/2\pi$. This statement should be contrasted with an estimate for χ obtained by resumming the RPA series with the g_4 term, i.e., $\chi \to (\chi^{-1} - g_4)^{-1}$. One can show that such resummation leads to a localized δ-function peak in $\mathrm{Im}\,\chi$, similarly to a recent work[6] where such a peak was demonstrated for $g_2=g_4$. However, in the presence of curvature, the RPA series does not exhaust all possible processes, as the multitail fermionic loops do not vanish, Eq. (12). Hence the result of simple RPA resummation is different from the answer by bosonization, which implies the multitail fermionic processes, particularly, the "drag diagrams," Fig. 2.

B. Curvature in Luttinger liquid

Let us discuss now the modification of the theory in the presence of the mixing interaction $\sim g_2 RL$ in Eq. (17). In this case right and left chiral densities mix, but the quadratic Hamiltonian which is the Luttinger model is still solvable.[12] The corresponding $u-v$ Bogoliubov transformation diagonalizes the Hamiltonian in terms of new chiral densities, $\tilde{R},\tilde{L}$, which obey the same commutation relations (20). Performing this transformation, one obtains

$$H_0 = \pi v(\tilde{R}^2 + \tilde{L}^2), \tag{30}$$

$$H_{cur} = \frac{\alpha_1}{3}(\tilde{R}^3 + \tilde{L}^3) + \frac{\alpha_2}{2}(\tilde{R}^2\tilde{L} + \tilde{R}\tilde{L}^2), \tag{31}$$

$$\alpha_1 = \frac{\pi^2}{m}\frac{3+K^2}{2\sqrt{K}}, \quad \alpha_2 = \frac{\pi^2}{m}\frac{(K^2-1)}{\sqrt{K}}, \tag{32}$$

with $v^2 = v_F(v_F + U/\pi)$, $K^2 = (1 + U/\pi v_F)^{-1}$. One can see from Eq. (31) that apart from some rescaling of the old mass term, $\tilde{R}^3 + \tilde{L}^3$, the effect of interaction gives rise to a new type of

curvature vertex, which mixes new right and left densities.

The density correlation function $\langle\rho\rho\rangle_{\omega q}$ is determined through the new variables $\tilde{R},\tilde{L}$ as

$$\langle\rho\rho\rangle_{\omega q} = K\langle(\tilde{R}+\tilde{L})(\tilde{R}+\tilde{L})\rangle_{\omega q}.$$

Note that RL mixing, which was removed at the level of quadratic action, reappears due to the curvature. The mixed terms $\langle\tilde{R}\tilde{L}\rangle$ are nonzero in the case of both $U\neq 0$ and $m^{-1}\neq 0$, and it necessitates the consideration of the (retarded) matrix Green's function

$$\tilde{G}(\omega,q) = \begin{pmatrix} \langle\tilde{R}\tilde{R}\rangle_{\omega q} & \langle\tilde{R}\tilde{L}\rangle_{\omega q} \\ \langle\tilde{L}\tilde{R}\rangle_{\omega q} & \langle\tilde{L}\tilde{L}\rangle_{\omega q} \end{pmatrix}.$$

It is clear that the PT for bosons in the case $K\neq 1$ contains processes absent in the free fermion case $K=1$.

Let us calculate the boson self-energy in the second order of PT. Denoting three types of boson loops as A_{RR},A_{RL},A_{LL}, one obtains

$$\Sigma_{RR} = 2\alpha_1^2 A_{RR} + \frac{1}{2}\alpha_2^2 A_{LL} + \alpha_2^2 A_{RL}, \tag{33}$$

$$\Sigma_{LL} = 2\alpha_1^2 A_{LL} + \frac{1}{2}\alpha_2^2 A_{RR} + \alpha_2^2 A_{RL}, \tag{34}$$

$$\Sigma_{RL} = \Sigma_{LR} = \alpha_1\alpha_2(A_{RR}+A_{LL}) + \alpha_2^2 A_{RL}. \tag{35}$$

Off the light cones, $\omega\neq\pm vq$, one has $\mathrm{Im}\,A_{RR}=\mathrm{Im}\,A_{LL}=0$ and all components of the imaginary part of the self-energy are given by the quantity

$$\Sigma_{off} \equiv \alpha_2^2 A_{RL}. \tag{36}$$

We list here the form of the appearing (retarded) expressions:

$$A_{RR} = \frac{1}{48\pi^3}\frac{q[q^2+(2\pi T/v)^2]}{qv-\omega-i0}, \tag{37}$$

$$A_{LL} = \frac{1}{48\pi^3}\frac{q[q^2+(2\pi T/v)^2]}{qv+\omega+i0}, \tag{38}$$

$$\mathrm{Im}\,A_{RL} = \frac{\pi}{2}\frac{\omega^2-v^2q^2}{(4\pi v)^3}\left[\coth\left(\frac{\omega+vq}{4T}\right)+\coth\left(\frac{\omega-vq}{4T}\right)\right]. \tag{39}$$

Note that the anomalous (appearing for $K\neq 1$ only) contribution A_{RL} is ultraviolet divergent, which will be reflected in the appearance of UV cutoff $\Lambda\sim E_F$ in the real part of A_{RL}. Seeking a function A_{RL}, analytical in the upper semiplane of ω, one can restore $\mathrm{Re}\,A_{RL}$ using the rule

$$i\coth\beta\omega \to -\frac{2}{\pi}\psi\left(-i\frac{\beta\omega}{\pi}\right)+\frac{1}{i\beta\omega}.$$

Such a recipe of analytical continuation delivers $\mathrm{Re}\,A_{RL}$ up to a constant $\sim\ln(T/\Lambda)$ multiplied by $(\omega^2-v^2q^2)$, as will be seen shortly.

In the limit of $T=0$, the expression for A_{RL} is simplified,

$$\mathrm{Im}\,A_{RL} = \pi\frac{\omega^2-v^2q^2}{(4\pi v)^3}\Theta(\omega^2-v^2q^2)\mathrm{sgn}\,\omega, \tag{40}$$

$$\mathrm{Re}\,A_{RL} = -\frac{1}{(4\pi v)^3}(\omega^2-v^2q^2)\ln\left|\frac{q^2v^2-\omega^2}{\Lambda^2}\right|. \tag{41}$$

Importantly, this part of Σ vanishes at the light cone for $T=0$ and remains finite (and purely imaginary) for $T\neq 0$, in contrast to the singular contributions A_{RR},A_{LL}. Notice the appearance of UV cutoff Λ in Eq. (41), which replaces temperature in this limit.

Neglecting for a moment the singular (purely real) parts A_{RR},A_{LL}, we write the Dyson equation in the form

$$\tilde{G}^{-1} = \begin{pmatrix} \tilde{g}_R^{-1}-\Sigma_{off} & -\Sigma_{off} \\ -\Sigma_{off} & \tilde{g}_L^{-1}-\Sigma_{off} \end{pmatrix}, \tag{42}$$

with $g_{R,L}^{-1}$ given by Eq. (21) with the change $v_F\to v$. Some calculation shows then that the Green's function defined for the initial fields ϕ,θ is given by

$$\begin{pmatrix} \langle\partial\phi,\partial\phi\rangle & \langle\partial\phi,\partial\theta\rangle \\ \langle\partial\theta,\partial\phi\rangle & \langle\partial\theta,\partial\theta\rangle \end{pmatrix} = \frac{\pi q^2}{\mathrm{Det}}\begin{pmatrix} Kv & \omega/q \\ \omega/q & K^{-1}(v-\Sigma_{off}/\pi) \end{pmatrix}, \tag{43}$$

with

$$\mathrm{Det} = q^2v^2-\omega^2-\frac{q^2v}{\pi}\Sigma_{off},$$

and ∂ standing for spatial derivative in Eq. (43).

As a result, the density correlations are given by

$$\langle\rho\rho\rangle_{\omega q} = \frac{1}{\pi^2}\langle\partial\phi\,\partial\,\phi\rangle_{\omega q} = \frac{Kvq^2/\pi}{q^2v^2-\omega^2-q^2v\Sigma_{off}/\pi} = \frac{v_F}{\pi}\frac{q^2Z}{q^2v^2-\omega^2}, \tag{44}$$

$$Z^{-1} = 1-\frac{q^2v\Sigma_{off}}{\pi(q^2v^2-\omega^2)}. \tag{45}$$

In the limit $T=0$ we have

$$Z^{-1} = 1-\gamma(q/k_F)^2\ln\frac{v^2q^2-(\omega+i0)^2}{\Lambda^2}, \tag{46}$$

$$\gamma = \frac{K(K^2-1)^2}{64}, \tag{47}$$

and $k_F=mv_F=Kmv$. The obtained logarithmic correction to the residue Z should be regarded as a first term in a series in m^{-1}. This correction is increasingly important at the energies close to the light-cone condition, $\omega\to v|q|$, and corresponds to the first term in the expansion of power-law singularity at $\omega\to v|q|$, which is discussed in Ref. 5.

Away from the light cone, when the real part of the logarithm in Z can be neglected, we obtain the contribution to the spectral weight at $\omega>0$:

$$\mathrm{Im}\,\langle\rho\rho\rangle_{\omega q} \simeq \frac{\gamma}{k_F^2}\frac{v_F q^4}{\omega^2 - q^2 v^2}\Theta(\omega^2 - v^2 q^2), \tag{48}$$

which shows a tail at higher energies, $|\omega| > |qv|$. This result was obtained earlier in Refs. 1, 3, and 4.

Finite temperatures, $T \gtrsim |\omega|, |qv|$, lead to the following modification:

$$\frac{q^2 v}{\pi}\Sigma_{off} \simeq i\gamma\frac{q}{k_F^2}4\pi\omega T, \tag{49}$$

and from Eq. (44) it appears that the bosonic excitations are characterized by damping

$$\omega \simeq \pm vq + 2i\pi\gamma T(q/k_F)^2. \tag{50}$$

However, this "damping" should not be viewed as the characteristic linewidth because it is smaller than the previous estimate for the width of the spectral width of the density correlator in the noninteracting case, $|\omega - vq| \sim Tq/k_F$. This wider spectral width comes from the omitted terms A_{RR}, A_{LL} which intervene close to the light cone condition $\omega = \pm vq$. The finite-T "damping" due to interaction manifests itself in the enhanced amplitude of the tails in the density correlator, and instead of Eq. (48) we obtain

$$\mathrm{Im}\,\langle\rho\rho\rangle_{\omega q} \simeq \frac{\gamma}{2k_F^2}\frac{v_F q^4}{(\omega^2 - q^2 v^2)}\left[\coth\left(\frac{\omega + vq}{4T}\right) + \coth\left(\frac{\omega - vq}{4T}\right)\right] \tag{51}$$

$$\simeq \frac{\gamma}{k_F^2}\frac{4v_F q^4 \omega T}{(\omega^2 - q^2 v^2)^2}, \tag{52}$$

which is parametrically larger than Eq. (48) at $|\omega - vq| \ll \omega \sim T$, and is nonzero also at $|\omega| < |qv|$. In the lowest order of intrawire interaction Eq. (51) was obtained in Ref. 4. It should be stressed again that Eqs. (48) and (51) are applicable only for $|\omega - vq| \gtrsim k_F^{-1}|q|\max(T, qv)$.

IV. ac CONDUCTIVITY OF SINGLE WIRE

Let us discuss the coupling to electromagnetic field in bosonization and its modification due to curvature. We start from a general expression for the kinetic term in the Hamiltonian,

$$\mathcal{H}_{kin} = \frac{1}{2m}\psi^\dagger(-i\nabla - eA)^2\psi - \mu\psi^\dagger\psi, \tag{53}$$

with $\hbar = c = 1$ and μ the chemical potential. Using the above representation $\psi(x) \sim e^{ik_F x + i\phi_R} + e^{-ik_F x - i\phi_L}$, and denoting

$$\Phi_R = k_F x + \phi_R, \quad \Phi_L = k_F x + \phi_L,$$

one can represent $\mathcal{H}_{kin}$ in the presence of eA as

$$\mathcal{H}_{kin} = \frac{1}{2\pi}\left[\frac{(\partial_x\Phi_R - eA)^3}{6m} - \mu\partial_x\Phi_R\right] + \frac{1}{2\pi}\left[\frac{(\partial_x\Phi_L + eA)^3}{6m} - \mu\partial_x\Phi_L\right]. \tag{54}$$

Slightly digressing here, we note that in this notation $k_F x$ is clearly a zero (classical) mode of the bosonic fields $\Phi_{R,L}$ which is obtained from Eq. (54) by variation over these fields. Note that the zero mode $k_F x$ corresponds to a local minimum of the action corresponding to Eq. (54), while the action is formally unstable with respect to a choice $\partial_x\Phi_{R,L} \to -\infty$. The latter unphysical choice of "classical" vacuum can be ruled out by imposing the hard-core condition, $\partial_x\Phi_{R,L} > 0$ for all x. It means that the local fluctuations of the density should not lead to negative values of total electronic density, $\partial_x\phi_R > -k_F$, etc. Quantizing these fluctuations around the classical vacuum as explained, e.g., in Ref. 19, one arrives to the above picture of Luttinger liquid plus cubic "interaction" terms. A similar approach was proposed earlier in Ref. 20.

Note that we can obtain Eq. (54) also by including vector potential in the U(1) phase according to $\psi(x) \sim e^{i\Phi_R - ie\int dxA} + e^{-i\Phi_L - ie\int dxA}$. The cubic terms in eA generated by two terms in Eq. (54) cancel each other. In a more general case of nonparabolic band dispersion, $\varepsilon(k)$, the Peierls substitution, $k \to k - eA$, leads to higher powers of eA in the gradient expansion of $\varepsilon(k - eA)$. The recipe for tackling this case was outlined long ago by Luttinger and Kohn[21] and amounts to retaining only eA and $(eA)^2$ terms in such an expansion, while discarding higher terms as unphysical.

Upon thermodynamic averaging of $\mathcal{H}_{kin}$, the diamagnetic term, $\sim(eA)^2$, gives the usual value, $k_F/(\pi m) = Kv/\pi$. This is the zero-mode contribution, whereas terms linear in $\partial_x\phi$ yield zero. The term linear in vector potential has a structure

$$\frac{eA}{2m}[(k_F + \partial_x\phi_L)^2 - (k_F + \partial_x\phi_R)^2] = \pi^{-1}eA(v_F\partial_x\theta + m^{-1}\partial_x\theta\partial_x\phi).$$

The last expression means that the electric current is given by the expression

$$j = -e\pi^{-1}(v_F\partial_x\theta + m^{-1}\partial_x\theta\partial_x\phi). \tag{55}$$

This expression is confirmed by the immediate application of the continuity equation, $\partial_x j = -\partial_t\rho = ie\pi^{-1}[\partial_x\phi, \mathcal{H}]$, and using the bosonized Hamiltonian (15). The first term in Eq. (55) is usual for LL, the second term appears due to the fluctuation of the Fermi velocity when changing the density.

The Kubo formula expresses the conductivity via the retarded Green's function of the uniform current,

$$\sigma(\omega) = \frac{\langle jj\rangle_{q=0,\omega} - \langle jj\rangle_{q=0,\omega=0}}{i\omega}. \tag{56}$$

The subtraction of the diamagnetic term $\langle jj\rangle_{q=0,\omega=0}$ should be performed when using direct representation (55). If one calculates first the density correlator and uses the continuity equation afterwards,

$$\langle jj\rangle_{q=0,\omega} = \lim_{q\to 0}\omega^2 q^{-2}\langle\rho\rho\rangle_{q,\omega},$$

then the diamagnetic contribution is subtracted automatically.

Using the above result, Eq. (44), we have

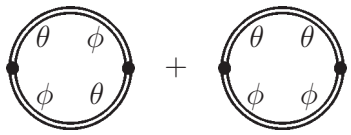

FIG. 4. Two boson loop diagrams formally contributing to ac conductivity. The labels $\theta\phi$, etc., at boson lines refer to the boson fields as discussed in text.

$$\sigma(\omega) = \frac{v_F}{-i\pi\omega}, \quad \mathrm{Re}\,\sigma(\omega) = v_F\delta(\omega); \tag{57}$$

i.e., the conductivity of *one wire* is not affected by the temperature, interaction, and curvature, in accordance with Giamarchi and Millis.[22] It should be stressed that this conclusion assumes our above choice $g_2=g_4=U$, i.e., physical charge-charge interaction; we do not consider models with $g_2 \neq g_4$ which would correspond to current-current interaction and to modifications of Eq. (57).

We also comment here on the equivalence of two ways of calculation of $\sigma(\omega)$, via Eq. (55) and via the continuity equation. Using Eq. (55) for the $\langle jj\rangle$ correlation function, one obtains a bosonic propagator $\langle\partial_x\theta,\partial_x\theta\rangle$, and bosonic loops of the form $m^{-2}\langle\partial_x\theta\partial_x\phi,\partial_x\theta\partial_x\phi\rangle$. From Eq. (43) the average $\langle\partial_x\theta,\partial_x\theta\rangle$ is vanishing in the limit $q\to 0$, and subtracting the diamagnetic contribution v_F/π, one arrives at Eq. (57). The bosonic loop terms give zero, as will be seen shortly.

The mixed terms in the $\langle jj\rangle$ correlator, $m^{-1}\langle\partial_x\theta,\partial_x\theta\partial_x\phi\rangle$, are zero in all orders of perturbation theory. It is trivial to see in lowest order of m^{-1} because the mixed average contains three bosons. In the next order, one has a diagram with a bosonic loop and the Green's function attached to it. This Green's function bears the zero external momentum and finite ω and hence vanishes. The same argument about zero contribution to conductivity can be applied to any diagram containing external lines carrying zero momentum, particularly in the two-wire situation. Hence apart from the δ-function contribution produced by conventional bosonization, we have to discuss only loop diagrams in Fig. 4 and their dressing by the interaction, m^{-1}.

V. ac CONDUCTIVITY, TWO WIRES

For the system described by the Hamiltonian (7), we wish to compute the transresistivity, i.e., the voltage drop in one wire, caused by the current in another wire. Technically, we use the Kubo formula and calculate the conductivity, not resistivity. We consider the drag effect which is caused purely by electronic interaction, and in the absence of disorder in wires. In this situation, one expects a δ-function contribution to the conductivity, which should be separated from the proper drag contribution, seen in the limit $\omega\to 0$. Let us first discuss this small-ω limit.

A. dc limit

A general form of transconductivity in the limit $\omega\to 0$ can be found when starting with the transresistivity matrix $\hat{R}(\omega)=[\hat{\sigma}(\omega)]^{-1}$. Exactly at $\omega=0$ the voltage drop in both wires should be absent when the drift charge velocities, $\pi j_i/k_{Fi}$, in both wires coincide. In order to see it suffices to make a Galilean transformation to the coordinate frame moving with the drift velocity.[1] We combine this observation with the third Newton law, equaling the forces acting on both wires, i.e., $E_1k_{F1}=-E_2k_{F2}$, with E_i the electric field induced in the ith wire, and represent the complex-valued impedance as a series in ω:

$$\hat{R}(\omega) = \pi r_0\begin{pmatrix} k_{F1}^{-2} & -k_{F1}^{-1}k_{F2}^{-1} \\ -k_{F1}^{-1}k_{F2}^{-1} & k_{F2}^{-2}\end{pmatrix} - i\omega\hat{A} + \omega^2\hat{A}_2 + \cdots, \tag{58}$$

with the transresistivity given by $R_{12}=\pi r_0/(k_{F1}k_{F2})$.

In the absence of interwire interaction U_{12} in Eq. (7), Eq. (57) shows that $r_0=0$, $\hat{A}_2=0$, and $\hat{A}=\pi\,\mathrm{diag}[v_{F1}^{-1},v_{F2}^{-1}]$. We make a natural conjecture, that $r_0,\hat{A}$, and $\hat{A}_2$ allow Taylor expansions in u. It follows then, that for $\omega \ll r_0 v_J k_F^{-2}$ the first two terms in Eq. (58) are of the order of $r_0k_F^{-2}$, and the third term is $\sim(r_0k_F)^{-2}O(u)$, i.e., it contains an additional small factor $O(ur_0)$. Therefore one can invert $\hat{R}(\omega)$at small ω, retaining only the first two terms in Eq. (58) and taking the above nonperturbed value of $\hat{A}$.

The resulting complex-valued conductivity is obtained as

$$\hat{\sigma}(\omega) = \hat{\sigma}_1(\omega) + \hat{\sigma}_2(\omega), \tag{59}$$

$$\hat{\sigma}_1(\omega) = \frac{\pi^{-1}d^{-1}}{+0-i\omega}\begin{pmatrix} v_{F1}v_{F2}^{-1}m_2^{-2} & m_1^{-1}m_2^{-1} \\ m_1^{-1}m_2^{-1} & v_{F1}^{-1}v_{F2}m_1^{-2}\end{pmatrix},$$

$$\hat{\sigma}_2(\omega) = \frac{\pi^{-1}d^{-1}}{r_0d-i\omega}\begin{pmatrix} m_1^{-2} & -m_1^{-1}m_2^{-1} \\ -m_1^{-1}m_2^{-1} & m_2^{-2}\end{pmatrix},$$

$$d = m_1^{-2}v_{F1}^{-1} + m_2^{-2}v_{F2}^{-1}. \tag{60}$$

Interestingly, Eq. (59) provides the universal, i.e., independent of details of fermionic interaction, relation between the drag resistivity and the drag conductivity in the small-ω limit,

$$R_{12}\,\mathrm{Re}\,[\sigma_{12}]|_{\omega\to 0} = (c+c^{-1})^{-2}, \tag{61}$$

with $c^2=m_1k_{F1}/(m_2k_{F2})$. The right-hand side of Eq. (61) is always less than 1/4, the latter value is achieved for equal wires.

In the continuum media, the integral of $\sigma(\omega)$ over all frequencies should not depend on the interactions in the system, this independence is known as the optical sum rule (see, e.g., Ref. 23 and references therein). From Eq. (59) we restore this statement:

$$\mathrm{Re}\int_{-O(r_0d)}^{O(r_0d)} d\omega\hat{\sigma}(\omega) \simeq \pi\begin{pmatrix} v_{F1} & 0 \\ 0 & v_{F2}\end{pmatrix}, \tag{62}$$

which means that the spectral weight of the part $\hat{\sigma}_2(\omega)$ is large at $\sim v_F$ and is concentrated at the lowest energies. Regrettably, this is the worst accessible region for bosonization analysis, as will be seen shortly.

We can cast Eq. (59) in the form

$$\hat{\sigma}(\omega)=\frac{\pi^{-1}}{-i\omega}\begin{pmatrix} v_{F1} & 0 \\ 0 & v_{F2}\end{pmatrix}+\frac{\pi^{-1}r_0}{\omega(\omega+ir_0d)} \times\begin{pmatrix} m_1^{-2} & -m_1^{-1}m_2^{-1} \\ -m_1^{-1}m_2^{-1} & m_2^{-2}\end{pmatrix}, \tag{63}$$

and identify the first term here with the bare bosons contribution (57), then the second term is entirely the effect of the curvature. At larger ω, we have the expansion

$$\mathrm{Re}\,\sigma\sim\frac{r_0m^{-2}}{\omega^2+r_0^2d^2}\propto\frac{r_0d}{\omega^2}-\frac{r_0^3d^3}{\omega^4}+\cdots.$$

The drag effect, $r_0d\neq 0$, is absent without curvature, and bosonization treats the curvature as perturbation. It means, particularly, that calculating the dc drag resistivity starting from the Kubo formula, (56), one should seek a lowest order contribution to Re $\sigma(\omega)$ behaving as ω^{-2}. Such a contribution should arise in the higher-than-second order of m^{-1}, and the next important term, ω^{-4}, is found in even higher order of PT. Our approach in determination of r_0 as the coefficient before the ω^{-2} term in conductivity is thus similar to memory function formalism.[24]

Below we prove that apart from the singular $\omega=0$ contribution, the matrix $\hat{\sigma}(\omega)$ is given by

$$\hat{\sigma}(\omega)=\sigma_d(\omega)\begin{pmatrix} m_1^{-2} & -m_1^{-1}m_2^{-1} \\ -m_1^{-1}m_2^{-1} & m_2^{-2}\end{pmatrix}. \tag{64}$$

This degenerate matrix cannot be inverted and one needs the complete representation (59) in order to obtain R_{12}. From now on we discuss the real part of the drag conductivity $\sigma_d(\omega)$.

B. Optical transconductivity

For the Hamiltonian (7), the bare Green's function defined for the vector $\Phi=(\partial_x\theta_1,\partial_x\phi_1,\partial_x\theta_2,\partial_x\phi_2)$ is found as

$$G=\pi\begin{pmatrix} v_{1J} & \omega/q & 0 & 0 \\ \omega/q & v_{1N} & 0 & U_{12}/\pi \\ 0 & 0 & v_{2J} & \omega/q \\ 0 & U_{12}/\pi & \omega/q & v_{2N}\end{pmatrix}^{-1}. \tag{65}$$

It shows that the excitation spectrum has two branches $\varepsilon_{+q}=v_+|q|$ and $\varepsilon_{-q}=v_-|q|$ with the sound (plasmon) velocities

$$v_\pm^2=\frac{1}{2}(v_1^2+v_2^2)\pm\sqrt{\frac{1}{4}(v_1^2-v_2^2)^2+u^2v_1^2v_2^2}, \tag{66}$$

we assume $v_+>v_->0$ below. We also focus on the case of almost identical wires, $v_1\simeq v_2=v$ and small u, when $v_+\simeq v_-\simeq v$ and

$$\Delta\equiv(v_+-v_-)/v_-\simeq\sqrt{(v_1-v_2)^2/v^2+u^2}\ll 1. \tag{67}$$

Let us discuss the first diagrams appearing in bosonization analysis of transconductivities. As shown above, the linear-in-boson components of the currents (55), $\partial\theta_i$, produce the δ-function contribution to the conductivity. This is the first term in Eq. (63).

The proper transconductivity part, $\sigma_d(\omega)$ in Eq. (64), is generated by the second term of the current operator in Eq. (55). Schematically, it is given by two diagrams, depicted in Fig. 4. These bosonization diagrams correspond to the usual fermionic ones, Fig. 2, after we identify Fig. 2 with Fig. 3 in the approach using the continuity relation, and notice that the external tail Green's function becomes constant in the limit $q\to 0$, $\omega\neq 0$.

After a lengthy calculation, sketched in the Appendix , we obtain

$$\sigma_d(\omega)=u^2\frac{\omega\sinh(\omega/2T)\ v_1^2v_2^2v_+^{-1}v_-^{-1}(v_++v_-)^{-5}}{8\sinh\left(\frac{v_+\omega}{2T(v_++v_-)}\right)\sinh\left(\frac{v_-\omega}{2T(v_++v_-)}\right)} +(v_-\to -v_-), \tag{68}$$

$$\sigma_d(0)=T\left(\frac{uv_1v_2}{v_+v_-}\right)^2\frac{v_+^3+3v_+v_-^2}{2(v_+^2-v_-^2)^3}. \tag{69}$$

The first observation about the obtained optical conductivity is that $\sigma_d(\omega)$ is nonzero solely due to the interwire interaction u. Second, at $\omega\gtrsim T$ the second term in Eq. (68) is exponentially small and the first one produces linear-in-ω optical conductivity,

$$\sigma_d(\omega)\sim u^2v_F\omega/E_F^2,\quad \omega\gtrsim T. \tag{70}$$

Unusually, there is no upper boundary for this regime in the theory, and Re $\sigma_d(\omega)\propto|\omega|$ until $|\omega|\ll E_F$. At the same time, the integral contribution of higher frequencies into the optical sum is small, $\int d\omega\,\sigma(\omega)\sim u^2v_F$, i.e., only a fraction of the above value (62).

In the case of identical wires, $v_1=v_2\equiv v$, coupled by a weak interaction, one has $u\ll 1$ and the new velocities $v_\pm=v\sqrt{1\pm u}$. The optical conductivity then takes the form

$$\sigma_d(\omega)\simeq\frac{u^2\omega\coth(\omega/4T)}{128v^3}+\frac{\omega\sinh(\omega/2T)}{8u^3v^3\sinh^2(\omega/2uT)}. \tag{71}$$

One sees the appearance of a smaller energy scale $uT\ll T$ in this case and parametric enhancement $\sigma_d(0)\sim T/u$; we return to this point below.

Overall, the function (68) is a smooth function of ω, not exhibiting the internal crossover at $\omega\sim r_0d\sim m^{-4}$ as suggested by Eq. (63). The region of applicability of the expression (68) can be estimated by using the "broadened" propagators (24) instead of δ-function-like (21), during calculation of $\sigma_d(\omega)$. This estimate shows that the finite bosons' linewidth becomes important in the formula (68) at $\omega\lesssim\omega_0=T^2/mv^2$, in accordance with Ref. 18. Using this estimate as a crossover energy from Eq. (68) to the Lorentzian form (63), we can write $\sigma_d(\omega_0)\simeq r_0/\omega_0^2$ and thus find r_0 up to a numerical coefficient. Remarkably, this simple method gives a correct value of r_0 at lowest T, but it wrongly estimates a crossover to the high-temperature regime, discussed below. We see that the estimate of r_0 requires going beyond the lowest order of curvature and we suggest a way to calculate it in the next section.

C. Alternative representation of $\sigma_d(\omega)$

In this section we derive another representation for $\sigma_d(\omega)$, which explicitly recovers the matrix structure (64) and shows the overall prefactor u^2 in $\sigma_d(\omega)$. For infinitesimal u this representation yields the well-known formula for the drag coefficient.

We rewrite the Kubo formula as

$$\sigma(\omega) = \frac{\langle \partial_t j \partial_t j \rangle_{q=0,\omega}}{i\omega^3} \tag{72}$$

and use the equation of motion $\partial_t j = i[\mathcal{H}, j]$ and Eq. (55). Some lengthy, but straightforward, calculation verifies that the commutation with the terms H_1, H_2, H_{cur} produces full derivatives with respect to x, which vanish for the uniform currents. The only surviving terms come from H_{12} in Eq. (7) and are

$$\partial_t j_1(x) = U_{12} m_1^{-1} \rho_1 \partial_x \rho_2, \tag{73}$$

$$\partial_t j_2(x) = U_{12} m_2^{-1} \rho_2 \partial_x \rho_1 \sim - U_{12} m_2^{-1} \rho_1 \partial_x \rho_2, \tag{74}$$

modulo full derivatives. It is immediately seen that the structure (64) is reproduced, and the scalar drag conductivity is given by

$$\sigma_d(\omega) = \frac{U_{12}^2}{i\omega^3} \langle \rho_1 \partial_x \rho_2, \rho_1 \partial_x \rho_2 \rangle_{q=0,\omega}. \tag{75}$$

Comparing to Eq. (63), we obtain at $\omega > r_0 d$

$$r_0 = \frac{U_{12}^2}{\omega} \mathrm{Im} \langle \rho_1 \partial_x \rho_2, \rho_1 \partial_x \rho_2 \rangle_{q=0,\omega}. \tag{76}$$

For the *infinitesimal* U_{12} the cross terms, $\sim \langle \rho_1, \partial_x \rho_2 \rangle$, in the average (75) can be neglected, and a comparison with Eq. (63) at $\omega \to 0$ gives

$$r_0 = \pi U_{12}^2 \int \frac{q^2 dq\, d\omega}{(2\pi)^2} \frac{\mathrm{Im}\, \chi_1(q,\omega) \mathrm{Im}\, \chi_2(q,\omega)}{2T \sinh^2(\omega/2T)}, \tag{77}$$

which corresponds to previous findings.[1,9] It is also worth noting that our Eq. (76) for transresistivity exactly corresponds to Eq. (18) in Ref. 25. We should stress, however, that the *exact formula* for the case of clean Luttinger liquids is given by Eq. (75) and Eq. (76) should be regarded as the high-energy asymptote of the expression (63).

D. Nonequal wires

We consider now the case of two wires, which are coupled by infinitesimal U_{12} and are characterized by nonequal plasmon velocites. In this case we can use Eq. (77) and the results of Sec. III B. In the absence of curvature and intrawire interaction, the formula (44) with $Z=1$ gives $r_0=0$ in Eq. (77). The first nonvanishing contribution is given by Eq. (51), and we obtain

$$r_0 = \frac{U_{12}^2 v_{F1} v_{F2}}{16\pi T (v_1^2 - v_2^2)} \int \frac{q^5 dq}{\sinh \frac{(v_1 - v_2)q}{4T} \sinh \frac{(v_1 + v_2)q}{4T}} \times \left[\frac{\gamma_2}{v_1 k_{F2}^2 \sinh(v_1 q/2T)} + (1 \leftrightarrow 2) \right]. \tag{78}$$

In the important case of almost identical wires, when $\Delta = (v_1 - v_2)/v \ll 1$, we can omit the wire index in the prefactors and expand $\sinh[(v_1 - v_2)q/4T] \simeq \Delta v q/4T$. Recalling that the transconductivity is $R_{12} = \pi r_0/(k_{F1} k_{F2})$, we obtain

$$R_{12} \simeq \frac{8\pi^4 U_{12}^2}{m^4 v^6 K^2 \Delta^2} \frac{\gamma T^5}{15 v^5}, \tag{79}$$

with γ given by Eq. (47), and we used $\int_{-\infty}^{\infty} dx x^4/\sinh^2 x = \pi^4/15$. Comparing Eq. (79) to the result by Pustilnik *et al.*,[1] we see that we obtained the same T^5 dependence but a parametrically larger prefactor, $(v_1 - v_2)^{-2}$, rather than $(v_1 - v_2)^{-1}$.

Note that one would reproduce the prefactor obtained in Ref. 1 if one neglected the T dependence of the density propagator and substituted in Eq. (77) the expression (48) for $\mathrm{Im}\, \chi_1(q,\omega)$ calculated at $T=0$, instead of Eq. (51). We see that finite T parametrically enhances the "tail" of the density correlator, and it has consequences for the drag effect. The importance of calculation of intermediate polarization operators $\mathrm{Im}\, \chi_i(q,\omega)$ in Eq. (77) at finite T was also emphasized in Ref. 10.

Checking the applicability of Eq. (51), one can conclude that the derivation of Eq. (79) assumed a condition $v_1 - v_2 \gtrsim T/k_F$. In other words, the expression (79) should be regarded as the *low-temperature* regime of drag resistivity, taking place at

$$T \ll T_1 \equiv k_F (v_1 - v_2) = E_F \Delta.$$

Above this temperature scale, the "core" spectral weights of $\chi_1''(q\omega)$ and $\chi_2''(q\omega)$ overlap and one can estimate the drag coefficient by taking the expression for the "core" of the density propagator for free fermions, Eq. (24), to obtain

$$R_{12} \sim \frac{U_{12}^2}{m v^5} T^2 F\left(\frac{T_1}{2T}\right), \tag{80}$$

with

$$F(z) = \int_0^\infty \frac{2x dx (x \coth x - z \coth z)}{\sinh(x+z)\sinh(x-z)},$$

$$= 1, \quad z \to 0,$$

$$\simeq 4 z^3 e^{-2z}/3, \quad z \gg 1.$$

The estimate (80) shows an activational behavior of the drag for free fermions, similarly to Ref. 1.

The obtained estimates for the drag effect at lower and higher temperatures, however, raise a few questions. First, Eqs. (80) and (79) apparently describe different contributions to the drag; they do not match at the suggested crossover

temperature $T \sim T_1$, and Eq. (79) is explicitly nonzero only due to intrawire interactions and this feature is absent in Eq. (80).

Second, in case of initially equal wires, the plasmon velocities are split due to interwire interaction, Eq. (67). It means that U_{12} cannot be regarded as infinitesimal in Eq. (75) and hence Eq. (78) is, generally speaking, invalid. In this case a naive substitution $\Delta \sim U_{12}/v$ from Eq. (67) results in independence of R_{12} from interwire coupling. To clarify these issues, we separately consider the case of nearly equal wires below.

VI. DRAG FOR NEARLY EQUAL WIRES IN BOSONIZATION

A. Identical wires, Hamiltonian

When the wires are identical, it is convenient to introduce the symmetrized combinations

$$\sqrt{2}\phi_\pm = \phi_1 \pm \phi_2, \quad \sqrt{2}\theta_\pm = \theta_1 \pm \theta_2. \tag{81}$$

A technical convenience of a $\sqrt{2}$ prefactor stems from the same commutation relations for the symmetrized operators, however, the zero modes are different, $\partial_x \phi_+^{(0)} = \sqrt{2}k_F$, $\partial_x \phi_-^{(0)} = 0$. We will call ϕ_+ and ϕ_- pseudocharge and pseudospin fields, by obvious analogy with bosonization for one wire in the spinful case.[12]

In terms of densities and momentum operators,

$$\rho_\pm = \pi^{-1}\partial_x \phi_\pm, \quad \Pi_\pm = \pi^{-1}\partial_x \theta_\pm, \tag{82}$$

the Hamiltonian (7) is rewritten as follows:

$$\mathcal{H} = \int dx (H_+ + H_- + H_{cur}), \tag{83}$$

$$H_\pm = \frac{\pi}{2}[v_J \Pi_\pm^2 + v_N(1 \pm u)\rho_\pm^2],$$

$$H_{cur} = \pi^2 \frac{\rho_+(\rho_+^2 + 3\Pi_+^2 + 3\Pi_-^2 + 3\rho_-^2) + 6\Pi_+\rho_-\Pi_-}{6m\sqrt{2}}. \tag{84}$$

It is seen that the change in the zero mode of ϕ_+ is compensated by the enhancement of its "mass." The plasmon velocities and Luttinger parameters are given by

$$v_\pm^2 = (1 \pm u)v_N v_J, \quad K_\pm^{-2} = (1 \pm u)v_N/v_J. \tag{85}$$

According to our definitions

$$K_\pm^{-2} = 1 + (\pi v_F)^{-1}(U_1 \pm U_{12}),$$

so that $K_- = 1$ for equal intrawire and interwire interactions.

We diagonalize the Hamiltonian (83) by transformation

$$\rho_\pm = K_\pm^{1/2}\tilde{\rho}_\pm, \quad \Pi_\pm = K_\pm^{-1/2}\tilde{\Pi}_\pm. \tag{86}$$

In terms of new left and right movers, $2\tilde{R}_\pm = \tilde{\rho}_\pm + \tilde{\Pi}_\pm$, $2\tilde{L}_\pm = \tilde{\rho}_\pm - \tilde{\Pi}_\pm$, there are no mixed terms $\tilde{R}_\pm \tilde{L}_\pm$ in $\mathcal{H}$, and propagators $\langle \tilde{R}_\pm \tilde{L}_\pm \rangle$ vanish.

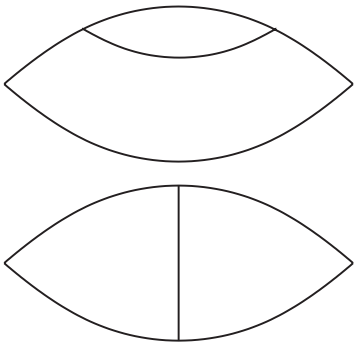

FIG. 5. Skeleton diagrams depicting the bosonic processes contributing to drag effect at lowest temperatures.

The curvature term becomes

$$H_{cur} = \frac{\alpha_1}{3}\left(\tilde{R}_+^3 + \tilde{L}_+^3\right) + \frac{\alpha_2}{2}\left(\tilde{R}_+^2\tilde{L}_+ + \tilde{R}_+\tilde{L}_+^2\right) + \frac{\alpha_3}{2}(\tilde{R}_+\tilde{R}_-^2 + \tilde{L}_+\tilde{L}_-^2)$$
$$+ \frac{\alpha_4}{2}(\tilde{R}_+\tilde{L}_-^2 + \tilde{L}_+\tilde{R}_-^2) + \alpha_5(\tilde{R}_+ + \tilde{L}_+)\tilde{R}_-\tilde{L}_-, \tag{87}$$

with

$$\alpha_1 = \frac{\pi^2}{m}\frac{3 + K_+^2}{2\sqrt{2K_+}}, \quad \alpha_2 = \frac{\pi^2}{m\sqrt{2}}\frac{(K_+^2 - 1)}{\sqrt{K_+}},$$

$$\alpha_{3(4)} = \frac{\pi^2\sqrt{K_+}}{m\sqrt{2}}\left(\frac{1}{K_-} + K_- \pm \frac{2}{K_+}\right),$$

$$\alpha_5 = \frac{\pi^2\sqrt{K_+}}{m\sqrt{2}}\left(K_- - \frac{1}{K_-}\right), \tag{88}$$

in the limit of vanishing interwire interaction we have $K_+ = K_-$ and $2\alpha_1 = \alpha_3$ and $\alpha_2 = \alpha_4 = \alpha_5$; this case returns us back to Eq. (31). In the absence of interaction, $K_\pm = 1$ and $\alpha_2 = \alpha_4 = \alpha_5 = 0$. Note that the vertex α_1, describing the decay within the same mode, is always nonzero.

The drag current operator in Eq. (75) is

$$\rho_1\partial_x\rho_2 = \rho_-\partial_x\rho_+ = (K_+K_-)^{1/2}\tilde{\rho}_-\partial_x\tilde{\rho}_+, \tag{89}$$

modulo full derivatives. We seek the contribution to r_0 in the next order in m^{-1} which can be obtained by considering two skeleton graphs, depicted in Fig. 5. The diagrams of the RPA type, Fig. 6, vanish, because in our case the intermediate propagator, connecting two boson loops, carries the zero external momentum and is zero at any external $\omega \neq 0$; see Eq. (21). Note that the external vertices in Figs. 5 and 6 correspond to Eq. (89) and do not contain m^{-1}, whereas the internal vertices correspond to Eq. (88), each bearing m^{-1}.

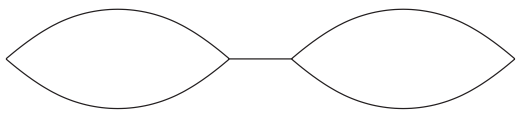

FIG. 6. RPA processes, which do not contribute to drag conductivity.

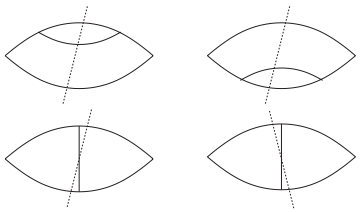

FIG. 7. Four cross sections corresponding to two above skeleton graphs.

Given ten possible decay processes (87), one has to analyze $\sim 10^2$ diagrams, corresponding to Fig. 5. It is further complicated by the necessity to perform the calculation at finite T and make an analytical continuation to real frequences $\omega \to 0$. Fortunately, there is a method which allows the essential simplification of this task.

B. Calculation by "Unitarity condition" method

At finite T, the analytical continuation of the diagrams and the essential reduction of their number under consideration are simultaneously achieved in the "Unitarity condition" method.[26] Since this method for $T>0$ is largely unknown to the wider audience, we sketch the main points of it below. Readers not interested in the details of calculation may skip to Eq. (98) below.

We define a cross section of the diagram as a line, bisecting this diagram in two parts, each with the external vertex $\rho_- \partial_x \rho_+$ carrying the external frequency ω (see Fig. 7). We should take the product of spectral weights of the Green's functions Im $g(x_i, q_i)$ at the cross section to divide each individual spectral weight by $2\sinh(x_i/2T)$ (in our case of bosons), and to multiply the whole product by $2\sinh(\omega/2T)$. The sum over all possible cross sections, multiplied by the square of the generalized vertex part, gives a value of the *imaginary part* of the diagram. See Figs. 8 and 9, schematically showing this method.

Using this method, all contributions can be classified by the number and type of Green's functions appearing in the cross section. Formally, we have the contributions with two propagators in the cross section (2-CS) and three propagators in the cross section (3-CS). However, the cross sections with two propagators are essentially reduced to the simple loop

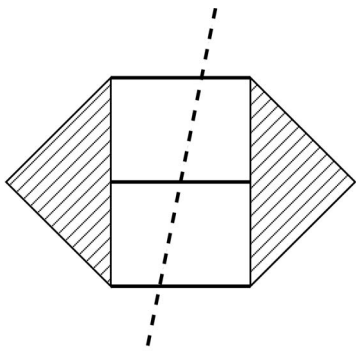

FIG. 8. The leading contribution to the low-T drag coefficient is given by diagrams with three propagators in a cross section.

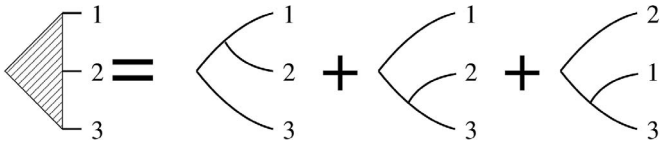

FIG. 9. First order in curvature contribution to the vertex part in the above diagram.

diagram, with a static vertex correction (except for diagrams with a α_1 vertex, see below). Given the structure of the external vertex, $\rho_- \partial_x \rho_+$, and kinematic properties for linear spectrum, one can verify that the contribution of 2-CS to σ does not contain ω^{-2}. We may hence exclude this type of cross section from our analysis.

Each partial 3-CS contribution to the drag resistivity can be represented as[26] [cf. Eq. (77)]

$$\delta r_0 = \pi U_{12}^2 K_+ K_- \int do |\Gamma_{jkl}|^2 S_{jkl}, \tag{90}$$

$$do = 2\pi^2 \delta\Big(\sum q_i\Big)\delta\Big(\omega - \sum x_i\Big)\prod_{i=1}^{3}\left[\frac{dq_i dx_i}{(2\pi)^2}\right],$$

$$S_{jkl} = \frac{g_j''(x_1,q_1) g_k''(x_2,q_2) g_l''(x_3,q_3)}{T \sinh\dfrac{x_1}{2T}\sinh\dfrac{x_2}{2T}\sinh\dfrac{x_3}{2T}}, \tag{91}$$

and the spectral weight $g_j''(x,q) = \mp(q/2)\delta(qv_j \pm \omega)$ is the imaginary part of the retarded Green's function for chiral density $j = \tilde{R}_\pm, \tilde{L}_\pm$, Eq. (21). A symmetrization prefactor 1/2 should be added to S_{jkl} when values of two indices are coinciding. The total drag resistivity is given by summation over all possible $j,k,l = R_\pm, L_\pm$ so that

$$r_0 = \pi U_{12}^2 K_+ K_- \sum_{jkl} \int \frac{dq_1 dq_2 dx_1 dx_2}{(2\pi)^2} |\Gamma_{jkl}|^2 \times \frac{g_j''(x_1,q_1) g_k''(x_2,q_2) g_l''(\omega - x_1 - x_2, -q_1 - q_2)}{2T \sinh\dfrac{x_1}{2T}\sinh\dfrac{x_2}{2T}\sinh\dfrac{x_1 + x_2 - \omega}{2T}}. \tag{92}$$

We can distinguish between the cross sections with (i) three different chiral densities, (ii) two different chiral densities, and (iii) one sort of chiral density.

(1) One sort of chiral density in the cross section can appear only on 3-CS of the type $g_{R-}'' g_{R-}'' g_{R-}''$ and $g_{L-}'' g_{L-}'' g_{L-}''$. The kinematic restrictions (91) obviously lead to the absence of such a contribution in Eq. (92) at $\omega \neq 0$.

Having this contribution excluded, we observe that the ω^{-2} contribution to σ is delivered by setting $\omega = 0$ in the integrand of Eq. (92); upon doing this the calculation is simplified.

(2) It can be shown that 3-CS with three different propagators may contain only two combinations $g_{R+}'' g_{L+}'' g_{L-}''$ and $g_{R+}'' g_{L+}'' g_{R-}''$. Summing up all the contributions, and using the

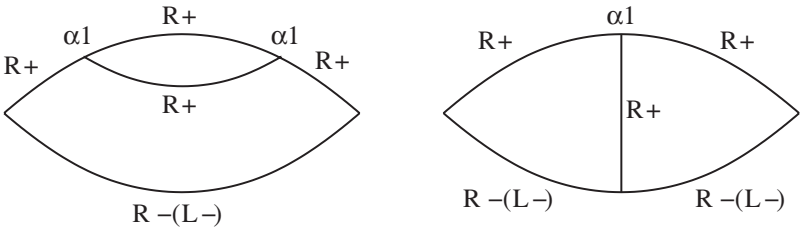

FIG. 10. Singular diagrams.

kinematic restrictions in do and S_{ijk}, Eq. (91), we obtain that the corresponding static vertex is

$$\Gamma_{R+L+L-} = \frac{q}{2\pi} \frac{4\alpha_2 v_+^2 + \alpha_3 (v_+ - v_-)^2 - \alpha_4 (v_+ + v_-)^2}{2v_+ (v_+^2 - v_-^2)}, \tag{93}$$

where q refers to the L_- boson; one has $\Gamma_{R+L+R-} = -\Gamma_{R+L+L-}$. The contribution to the drag coefficient is proportional to

$$\int \frac{dqq^3 |\Gamma_{R+L+L-}|^2 (v_+^2 - v_-^2) v_+^{-3}}{T \sinh \frac{(v_+ - v_-)q}{4T} \sinh \frac{(v_+ + v_-)q}{4T} \sinh \frac{v_- q}{2T}}; \tag{94}$$

this expression corresponds to Eq. (78). However, substituting Eq. (88) into Eq. (93), one obtains $\Gamma_{R+L+L-}=0$ and the absence of this partial contribution to r_0 (cf. next section).

(3) The remaining combinations, i.e., 3-CS with two different propagators, are $g''_{R-}g''_{R-}g''_{L-}$, $g''_{R+}g''_{R+}g''_{R-}$, $g''_{R+}g''_{R+}g''_{L-}$, and the combinations which are obtained from the above ones by the change $R \leftrightarrow L$. Due to obvious symmetry, the latter change together with $q_i \to -q_i$ leaves the expressions for δr_0 intact, so it suffices to consider only the above three CSs and multiply the result by two.

The first cross section, $g''_{R-}g''_{R-}g''_{L-}$, corresponds to the nonvanishing vertex

$$\Gamma_{R-R-L-} = \frac{q_1}{2\pi} \frac{2\alpha_5 v_+}{v_+^2 - v_-^2}, \tag{95}$$

where the kinematic restrictions were used again.

Finally, we come to the most problematic term of the cross sections $g''_{R+}g''_{R+}g''_{R-}$ and $g''_{R+}g''_{R+}g''_{L-}$. The corresponding vertices Γ's in Eq. (90), Fig. 9, explicitly read as

$$\begin{aligned} \Gamma_{R+R+R-} = {} & \alpha_1 q_3 g_{R+}(x_1 + x_2, q_1 + q_2) \\ & + \alpha_2 q_3 g_{L+}(x_1 + x_2, q_1 + q_2) \\ & - \alpha_3 q_1 g_{R-}(x_2 + x_3, q_2 + q_3) \\ & - \alpha_5 q_1 g_{L-}(x_2 + x_3, q_2 + q_3), \end{aligned} \tag{96}$$

$$\begin{aligned} \Gamma_{R+R+L-} = {} & \alpha_1 q_3 g_{R+}(x_1 + x_2, q_1 + q_2) \\ & + \alpha_2 q_3 g_{L+}(x_1 + x_2, q_1 + q_2) \\ & - \alpha_5 q_1 g_{R-}(x_2 + x_3, q_2 + q_3) \\ & - \alpha_4 q_1 g_{L-}(x_2 + x_3, q_2 + q_3). \end{aligned} \tag{97}$$

It is seen here that the term $\sim \alpha_1$ is divergent on the assumption of ideal bosons, which happens because of simultaneous conservation of energy and momentum for the linearized spectrum. This divergence in $g_{R+}(x_1+x_2, q_1+q_2)$ would not happen if we would assume a damping of boson excitations; moreover, the kinematic restrictions in the cross section (91) lead to prefactor $q_3=0$ at $\omega=0$, so that the contribution from the α_1 term is zero for any model damping of bosons. In our problem, however, this "damping" can only be obtained as the result of resummation of higher order corrections in m^{-1}. The divergent diagrams are depicted in Fig. 10.

The first diagram here, $\sim \alpha_1^2$, is the lowest order contribution to the self-energy part, Eq. (28). Evidently it corresponds to the triple pole $(x - v_+ q)^{-3}$ which resulted in the above divergence. At the same time, as discussed above, this is the first singular diagram in a series, which should ultimately produce the broadened propagator, Eq. (24). Importantly, this type of singular diagrams appears without the properly fermionic interaction, as seen in Eq. (88). Therefore, in the application of the formula (92), one should omit the most singular contribution, $\sim \alpha_1^2$, in $|\Gamma_{R+R+R-}|^2$ and use the broadened propagator, Eq. (24), instead.

The subleading singular term, $\sim \alpha_1$, is depicted by the right diagram in Fig. 10. We argue here that this diagram should vanish in our consideration, and provide the following heuristic argument. The linear dispersion law for bosons led to the singularity in the α_1 term (96), but this singularity is removed on the assumption of finite width of the bosonic pole. In this case the Green's function $g_{R+}(x_1+x_2, q_1+q_2)$ in Eqs. (96) and (97) becomes a purely imaginary quantity. Considering the purely real $|\Gamma_{R+R+R-}|^2 = \Gamma^*_{R+R+R-}\Gamma_{R+R+R-}$ one sees that the linear-in-α_1 terms disappear. This argument is most obvious for the simple Lorentzian form of $g_{R+}(x,q)$ and should be generalized for more complicated cases, particularly, for $g_{R+}(x,q)$ given by Eq. (24). The analytical structure of more complicated diagrams at finite T becomes rather involved, see Ref. 26, and a general proof of the cancellation of these vertex corrections should be considered elsewhere. Here we make a conjecture that the singular terms represented by the second diagram in Fig. 10 vanish exactly for the "dressed" propagators, given by Eq. (24).

This conjecture basically amounts to the following convention:

(i) one should discard the curvature term α_1 from the Hamiltonian;

(ii) one should use the dressed propagators (24) for the modes R_+, L_+, with the "effective mass" $1/m^* = \alpha_1/(2\pi^2)$, and plasmon velocity v_+ instead of v_F; and

(iii) the other curvature terms $\alpha_2, \ldots, \alpha_5$, not leading to singularities, can be treated in the regular PT.

Proceeding this way, we conclude that at higher temperatures, $T \gtrsim T_1$, we can use Eq. (78) with the change $\mathrm{Im}\,\chi_1\,\mathrm{Im}\,\chi_2 \to \mathrm{Im}\,\chi_+\,\mathrm{Im}\,\chi_-$. The finite width of the dressed propagators g_{R+}, g_{L+} then leads to the regime $r_0 \sim T^2$, similar to Eq. (80).

The interaction-induced corrections[5] to the shape of propagator (24) are the next-order effect in curvature, and do not influence our calculation of r_0 below. Indeed, at lowest temperatures, $T \ll T_1$, the peaks in spectral weights Im χ_i in Eq. (78) do not overlap, and it suffices to consider the "tail" of one propagator in Eq. (78) and the core of another one, approximated by the δ function. At higher temperatures, $T \gtrsim T_1$, propagators in Eq. (78) significantly overlap; this is a nonperturbative regime for bosonization, which cannot provide a prefactor in the estimate $r_0 \sim T^2$. However, one may argue that all interaction-induced details[5] in the shape of the core of propagators are smeared by higher temperatures and one can safely use the free-fermion estimate (24) here.

At lower temperatures, $T \ll T_1$, we obtain the finite contribution $r_0 \sim T^5$, due to vertices $\alpha_2, \ldots, \alpha_5$, absent in the noninteracting situation. A rather long and straightforward calculation gives a prefactor in this T^5 temperature dependence:

$$r_0 = U_{12}^2 \gamma T^5, \quad \gamma = \gamma_1 + \gamma_2 + \gamma_3,$$

$$\gamma_1 = \frac{1}{4\pi^2} \frac{[\alpha_3(v_+ + v_-) - \alpha_5(v_+ - v_-)]^2}{30 v_+^5 v_-(v_+ - v_-)(v_+^2 - v_-^2)^2},$$

$$\gamma_2 = \frac{1}{4\pi^2} \frac{[\alpha_5(v_+ + v_-) - \alpha_4(v_+ - v_-)]^2}{30 v_+^5 v_-(v_+ + v_-)(v_+^2 - v_-^2)^2},$$

$$\gamma_3 = \frac{1}{4\pi^2} \frac{\alpha_5^2 v_+^2}{15 v_-^7 (v_+^2 - v_-^2)^2}, \tag{98}$$

with α_j given by Eq. (88). It is seen that at $v_+ - v_- \to 0$ the leading term in γ is given by the α_3^2 term and is $\propto (v_+ - v_-)^{-3}$, which is different from the above regime $\sim (v_+ - v_-)^{-2}$ nonequal wires, Eq. (79). To resolve the seeming discrepancy, we perform the analysis of the nearly equal wires below.

C. Nearly identical wires

We consider now the case when the plasmon velocities $v_{1,2}$ in individual wires are nearly coinciding and their difference is of the order of U_{12}. The main idea of this section is that the coefficients in the canonical transformation diagonalizing the quadratic Luttinger Hamiltonian are sensitive to the ratio $U_{12}/(v_1 - v_2)$. These coefficients, in turn, define the values α_i for the vertices (87). We can calculate these values and use the previous expressions (94) and (98) to obtain the drag in this more general case.

Using the dimensionless difference of plasmon velocities (67), it is convenient to introduce the parameter λ as follows:

$$u = \Delta \sin \lambda, \quad v_1 - v_2 \simeq v \Delta \cos \lambda, \tag{99}$$

where the first equality is the proper definition of λ.

The general Bogoliubov transformation, diagonalizing the quadratic part of the Hamiltonian (7), explicitly reads as

$$\begin{pmatrix} \theta_1 \\ \theta_2 \\ \phi_1 \\ \phi_2 \end{pmatrix} = S_1 S_2 S_3 \begin{pmatrix} \theta_+ \\ \theta_- \\ \phi_+ \\ \phi_- \end{pmatrix}, \tag{100}$$

with

$$S_1 = \mathrm{diag}[v_{J1}^{-1/2} \quad v_{J2}^{-1/2} \quad v_{J1}^{1/2} \quad v_{J2}^{1/2}],$$

$$S_3 = \mathrm{diag}[v_+^{1/2} \quad v_-^{1/2} \quad v_+^{-1/2} \quad v_-^{-1/2}],$$

$$S_2 = \begin{pmatrix} \cos(\lambda/2) & -\sin(\lambda/2) & 0 & 0 \\ \sin(\lambda/2) & \cos(\lambda/2) & 0 & 0 \\ 0 & 0 & \cos(\lambda/2) & -\sin(\lambda/2) \\ 0 & 0 & \sin(\lambda/2) & \cos(\lambda/2) \end{pmatrix},$$

where v_+ and v_- are given by Eq. (66) and correspond to the new modes ϕ_+ and ϕ_-, respectively. Using this transformation, we can determine the values of the coefficients α_i in Eq. (87).

Note that the set of vertices (87) was obtained for the case $\lambda = \pi/2$. For other values of λ, we have also another set of the vertices which is obtained from Eq. (87) by a change $R_+ \leftrightarrow R_-$ and $L_+ \leftrightarrow L_-$, explicitly

$$H'_{cur} = \frac{\alpha'_1}{3}(\tilde{R}_-^3 + \tilde{L}_-^3) + \frac{\alpha'_2}{2}(\tilde{R}_-^2 \tilde{L}_- + \tilde{R}_- \tilde{L}_-^2) + \frac{\alpha'_3}{2}(\tilde{R}_- \tilde{R}_+^2 + \tilde{L}_- \tilde{L}_+^2)$$
$$+ \frac{\alpha'_4}{2}(\tilde{R}_- \tilde{L}_+^2 + \tilde{L}_- \tilde{R}_+^2) + \alpha'_5(\tilde{R}_- + \tilde{L}_-)\tilde{R}_+ \tilde{L}_+. \tag{101}$$

For our purposes here, it is sufficient to let $v_{J1} = v_{J2}$ and $s_1 \simeq s_2$ in the calculation of α_j, α'_j. Thus we neglect the difference in plasmon velocities in Eq. (100). At the same time, we allow for the intrawire interaction, $K = v_{J1}/s_1 \neq 1$.

We obtain the expressions for vertices in Eq. (87) as

$$\alpha_1 \simeq \frac{\pi^2}{m} \frac{3 + K^2}{2\sqrt{K}} \left(\cos^3 \frac{\lambda}{2} + \sin^3 \frac{\lambda}{2} \right),$$

$$\alpha_2 \simeq \frac{\pi^2}{m} \frac{K^2 - 1}{\sqrt{K}} \left(\cos^3 \frac{\lambda}{2} + \sin^3 \frac{\lambda}{2} \right),$$

$$\alpha_3 \simeq \frac{\pi^2}{m} \frac{K^2 + 3}{2\sqrt{K}} \left(\cos \frac{\lambda}{2} + \sin \frac{\lambda}{2} \right) \sin \lambda,$$

$$\alpha_4 \simeq \frac{\pi^2}{m} \frac{K^2 - 1}{2\sqrt{K}} \left(\cos \frac{\lambda}{2} + \sin \frac{\lambda}{2} \right) \sin \lambda,$$

$$\alpha_5 \simeq \alpha_4, \tag{102}$$

and the set α'_j is obtained from Eq. (102) by changing $\alpha_j \to \alpha'_j$ and $\lambda \to -\lambda$. The previous expressions (88) are restored by putting $\lambda = \pi/2$ in Eq. (102).

One can verify that despite a more complicated structure Eq. (100), the drag current vertex is still given by the last expression in Eq. (89). Further, the existence of the second set of vertices, α'_j, leads to the same set of diagrams as

before, with appropriate change $R_+ \leftrightarrow R_-$, etc. Importantly, there are no diagrams of the type Fig. 5, containing both α_j' and α_j. It means that one can use the previous expressions (98), corroborated by the previously vanishing contribution (94) and add the contribution from the α_j' set, obtained by $\lambda \to -\lambda$.

Combining all terms, we find

$$r_0 \simeq \frac{\pi^3 K U_{12}^2 T^5}{120 m^2 v^9}\left[\frac{(1-K^2)^2\cos^2\lambda}{\Delta^2}+\frac{(3+K^2)^2\sin^2\lambda}{4\Delta^3}\right]$$
$$\sim \frac{U_{12}^2 T^5}{E_F^2 v_F^5}\left(\frac{\cos^2\lambda}{\Delta^2}O(1)+\frac{\sin^2\lambda}{\Delta^3}O(1)\right). \quad (103)$$

This is the central result of this section. Let us discuss it in more detail.

First of all, we see that the term $\sim\Delta^{-2}$ in Eq. (103) is proportional to intrawire interaction strength, $(1-K)^2$, whereas the term $\sim\Delta^{-3}$ is present even for initially noninteracting wires. This is not surprizing, because in the latter case the factor $\sin^2\lambda \sim U_{12}^2/(v_1-v_2)^2$ means that U_{12} serves as the Luttinger-type interaction $(K-1)$; this term should be obtained for nonequal wires in the order U_{12}^4 of conventional fermionic formalism.

For identical wires, we have an interesting crossover from the $U_{12}^2T^2$ regime at high temperatures to $T^5/|U_{12}|$ behavior at lower temperatures. Recalling our definitions of the drag resistivity $R_{12}=\pi r_0/(k_{F1}k_{F2})$ and of the small scale $T_1 = E_F\Delta \sim U_{12}k_F$, we obtain

$$R_{12} \sim \frac{T^5}{v_F E_F^3 T_1}, \quad T < T_1,$$
$$\sim U_{12}k_F \sim \frac{T_1^2 T^2}{v_F E_F^3}, \quad T > T_1, \quad (104)$$

which shows a smooth crossover at $T \simeq T_1$. The parametrically large prefactor, $1/U_{12}$, is similar to above Eq. (71). This prefactor (i) shows nonperturbative character of the obtained result and (ii) does not mean actual enhancement of the drag effect, due to its overall small amplitude $\sim T^5$.

For the wires with different plasmon velocities we have $T_1 \simeq (v_1-v_2)k_F$, and the above Eq. (103) shows the following behavior:

$$R_{12} \sim \frac{T^5}{v_F E_F^2 T_1^2}\frac{U_{12}^2(1-K)^2}{v_F^2}, \quad T < T_1,$$
$$\sim \frac{U_{12}^2 T^2}{v_F^3 E_F}, \quad T > T_1, \quad (105)$$

and two regimes do not match at $T=T_1$. As we saw above, the T^2 regime changes to an exponential decrease at $T<T_1$, which means that there is a logarithmically narrow crossover region of temperatures, where R_{12} interpolates between T^5 and T^2 in Eq. (105).

VII. SUMMARY AND CONCLUSIONS

In this paper we discuss the effects of curvature for the Luttinger liquid. The curvature is irrelevant perturbation, in the sense that it does not change the low-energy sector of the system and usually can be simply discarded. The bosonization technique regards the curvature as interaction and, at the first glance, a regular perturbation theory is possible. However, certain care must be exercised with such PT, in spite of evident correspondence between fermionic and bosonization results. We show that the PT in curvature in bosonization produces both singular and regular contributions to different quantities. The singular contributions arise already for the free fermions and correspond to the non-Lorentzian character of the fermionic density propagator. We show that these singular contributions stem from one vertex of boson interaction, and we propose to exclude this vertex from PT analysis, while simultaneously using the free-fermion expression as a "dressed" form of bosonic propagators. For the Coulomb drag problem, the dressed form of propagators becomes important at high temperatures.

All other bosonic vertices appear due to fermionic interaction and yield regular contributions in bosonization PT. They are responsible for the low-T regime in the Coulomb drag problem.

Comparing bosonization to the fermionic approach in the example of a Coulomb drag problem, we observe a complementary character of these methods. The high-temperature T^2 regime is obtained most easily with fermions, but this is essentially a nonperturbative regime for bosonization. Conversely, the low-temperature T^5 drag regime for different wires is obtained relatively easily with bosons, whereas the calculation by the fermionic approach is cumbersome. We demonstrated that the bosonization is particularly useful in case of Coulomb drag between nearly equal wires, when it simultaneously resums several RPA channels for fermionic diagrams.

We did not include spin into our consideration. It also requires a separate analysis, because the cubic terms in the fermionic densities violate the spin-charge separation realized at the level of quadratic action. It is evident that spinful electrons in one wire are equivalent to spinless fermions in two wires. In our formalism, the Hamiltonian is given by Eq. (83) with identification ϕ_+ (ϕ_-) for charge (spin) density. The above case of nearly identical wires corresponds to Zeeman splitting of the Fermi velocities in the magnetic field by value $\sim B/k_F$.

Finally, we note that in one spatial dimension, the alternative source for the "ideal" drag was proposed by Nazarov and Averin.[11] They considered the "backscattering" between the wires, i.e., $2k_F$ Fourier component of the interwire interaction $U_{12}(2k_F)=U_{bs}$, not considered here. The effect of renormalization leads to the increase $\bar{U}_{bs}=U_{bs}(E_F/T)^{2-2K}$ with lowering T, and the drag resistivity $R_{12}\sim\bar{U}_{bs}^2$ diverges in the limit $T\to 0$. However, as was noted in Refs. 1 and 27, for large interwire distances D, the backscattering amplitude is small $U_{12}^{bs}\sim e^{-2k_F D}$ and the effect of renormalization can compensate this smallness only at exponentially small temperatures. The backscattering drag mechanism is also sensitive to the difference of fermionic densities in two wires.[11,27] Particularly, a straightforward calculation by Fuchs *et al.*[27] showed the exponential suppression of R_{12} due to backscattering at $T<v_F(k_{F1}-k_{F2})=T_1^*$. In view of an obvious

similarity between T_1^* and our T_1, it is tempting to regard the regime $R_{12} \sim T^5$ as the only one, surviving at low temperatures. The inclusion of the backscattering drag mechanism into our discussion is clearly beyond the scope of this study.

ACKNOWLEDGMENTS

I thank L. I. Glazman, M. Pustilnik, A. Luther, A. Kamenev, P. Kopietz, D. G. Polyakov, S. Teber, and A. G. Yashenkin for numerous useful discussions. I am very grateful to I. V. Gornyi and A. D. Mirlin for intensive discussions at the final stage of this work and valuable comments on the draft.

APPENDIX: OPTICAL CONDUCTIVITY

We calculate optical transconductivity according to the Kubo formula, Eq. (56), and have $\mathrm{Re}\,\hat{\sigma}_{jl}=\omega^{-1}\,\mathrm{Im}\,Q_{jl}(\omega)$ where $Q_{jl}(\omega)$ is a retarded current response function. Combining different contributions to $\hat{Q}(\omega)$, depicted in Fig. 4 and making an analytical continuation to real frequencies at finite T, we obtain

$$Q_{jl} = \int dq dx_1 dx_2 F_{jl} \frac{N(x_1) - N(x_2)}{\omega - x_1 + x_2 + i0} W(x_1) W(x_2),$$

$$F_{12} = F_{21} = \frac{1}{2} q^6 u^2 v_1^2 v_2^2 (x_1 + x_2)^2, \tag{A1}$$

$$F_{11} = q^2 (x_1^2 - v_2^2 q^2)(x_2^2 - v_2^2 q^2)(x_1 x_2 + v_1^2 q^2) + \frac{1}{2} q^6 u^2 v_1^2 v_2^2 (x_1^2 + x_2^2 - 2 v_2^2 q^2), \tag{A2}$$

$$W(x) = \frac{1}{2x(\varepsilon_1^2 - \varepsilon_2^2)} [\delta(x + \varepsilon_1) + \delta(x - \varepsilon_1) - \delta(x + \varepsilon_2) - \delta(x - \varepsilon_2)], \tag{A3}$$

and F_{22} is obtained from F_{11} by interchanging v_1 and v_2; here $N(x)$ is a Planck function.

We calculate $\mathrm{Im}\,Q_{12}$ at $\omega \neq 0$. For nonzero frequencies the coinciding arguments $x_1 = x_2 = \pm \varepsilon_{1,2}$ do not contribute and the rest of the integration is simple. After collecting all the terms coming from Eq. (A3) we obtain the real part of the conductivity $\mathrm{Re}\,\hat{\sigma}(\omega)$ in the form (64), with σ_d given by Eq. (68).

*On leave from Petersburg Nuclear Physics Institute, Gatchina 188300, Russia.

[1] M. Pustilnik, E. G. Mishchenko, L. I. Glazman, and A. V. Andreev, Phys. Rev. Lett. **91**, 126805 (2003).

[2] A. G. Abanov and P. B. Wiegmann, Phys. Rev. Lett. **95**, 076402 (2005).

[3] R. G. Pereira, J. Sirker, J.-S. Caux, R. Hagemans, J. M. Maillet, S. R. White, and I. Affleck, Phys. Rev. Lett. **96**, 257202 (2006).

[4] S. Teber, Eur. Phys. J. B **52**, 233 (2006); Phys. Rev. B **76**, 045309 (2007).

[5] M. Pustilnik, M. Khodas, A. Kamenev, and L. I. Glazman, Phys. Rev. Lett. **96**, 196405 (2006).

[6] P. Pirooznia and P. Kopietz, arXiv:cond-mat/0512494 (unpublished).

[7] M. Pustilnik, Phys. Rev. Lett. **97**, 036404 (2006); D. B. Gutman, arXiv:cond-mat/0608448; D. B. Gutman, arXiv:cond-mat/0612234.

[8] A. G. Rojo, J. Phys.: Condens. Matter **11**, R31 (1999); P. Debray, V. N. Zverev, V. L. Gurevich, R. Klesse, and R. S. Newrock, Semicond. Sci. Technol. **17**, R21 (2002).

[9] A.-P. Jauho and H. Smith, Phys. Rev. B **47**, 4420 (1993); L. Zheng and A. H. MacDonald, *ibid.* **48**, 8203 (1993); K. Flensberg, Ben Yu-Kuang Hu, A.-P. Jauho, and J. M. Kinaret, *ibid.* **52**, 14761 (1995); A. Kamenev and Y. Oreg, *ibid.* **52**, 7516 (1995).

[10] I. V. Gornyi, A. D. Mirlin, and F. von Oppen, Phys. Rev. B **70**, 245302 (2004).

[11] Yu. V. Nazarov and D. V. Averin, Phys. Rev. Lett. **81**, 653 (1998).

[12] A. O. Gogolin, A. A. Nersesyan, and A. M. Tsvelik, *Bosonization and Strongly Correlated Systems* (Cambridge University Press, Cambridge, England, 1998).

[13] F. D. M. Haldane, J. Phys. C **14**, 2585 (1981).

[14] M. Schick, Phys. Rev. **166**, 404 (1968).

[15] S. Tomonaga, Prog. Theor. Phys. **5**, 544 (1950).

[16] I. E. Dzyaloshinskii and A. I. Larkin, Sov. Phys. JETP **38**, 202 (1974).

[17] A. Neumayr and W. Metzner, J. Stat. Phys. **96**, 613 (1999).

[18] K. V. Samokhin, J. Phys.: Condens. Matter **10**, L533 (1998).

[19] D. N. Aristov and A. Luther, Phys. Rev. B **65**, 165412 (2002).

[20] A. Gramada and M. E. Raikh, Phys. Rev. B **55**, 1661 (1997).

[21] J. M. Luttinger and W. Kohn, Phys. Rev. **97**, 869 (1955).

[22] T. Giamarchi and A. J. Millis, Phys. Rev. B **46**, 9325 (1992).

[23] D. N. Aristov and R. Zeyher, Phys. Rev. B **72**, 115118 (2005).

[24] W. Götze and P. Wölfle, Phys. Rev. B **6**, 1226 (1972).

[25] I. D'Amico and G. Vignale, Phys. Rev. B **62**, 4853 (2000).

[26] S. V. Maleyev, Theor. Math. Phys. **4**, 694 (1970).

[27] R. Klesse and A. Stern, Phys. Rev. B **62**, 16912 (2000); T. Fuchs, R. Klesse, and A. Stern, *ibid.* **71**, 045321 (2005).